Hindawi
Complexity
Volume 2020, Article ID 7892362, 12 pages
https://doi.org/10.1155/2020/7892362

Research Article

Spatiotemporal Characteristics of Urban Surface Temperature and Its Relationship with Landscape Metrics and Vegetation Cover in Rapid Urbanization Region

Hongbo Zhao,[1] Juntao Tan,[2] Zhibin Ren,[3] and Zheye Wang[4]

[1]*Key Research Institute of Yellow River Civilization and Sustainable Development & Collaborative Innovation Center on Yellow River Civilization of Henan Province, Henan University, Kaifeng 475001, Henan, China*
[2]*School of Geography, Geomatics and Planning, Jiangsu Normal University, Xuzhou 221116, China*
[3]*Key Laboratory of Wetland Ecology and Environment, Northeast Institute of Geography and Agroecology, Chinese Academy of Sciences, Changchun, Jilin 130102, China*
[4]*Department of Environmental Sciences, College of the Coast and Environment, Louisiana State University, Baton Rouge, LA 70803, USA*

Correspondence should be addressed to Juntao Tan; tanjuntaocf@163.com and Zhibin Ren; renzhibin@iga.ac.cn

Received 21 April 2020; Revised 12 June 2020; Accepted 18 June 2020; Published 27 July 2020

Guest Editor: Jun Yang

Under the trend of rapid urbanization, the urban heat island (UHI) effect has become a hot issue for scholars to study. In order to better alleviate UHI effect, it is important to understand the effect of landuse/landcover (LULC) and landscape patterns on the urban thermal environment from perspective of landscape ecology. This research aims to quantitatively investigate the effect of LULC landscape patterns on UHI effects more accurately based on a landscape metrics analysis. In addition, we also explore the complex relationship between land surface temperature (LST) and vegetation cover. Taking Zhengzhou City of China as a case study, an integrated method which includes the geographic information system (GIS), remote-sensing (RS) technology, and landscape metrics was employed to facilitate the analysis. Landsat data (2000–2014) were applied to investigate the spatiotemporal evolution patterns of LST and LULC. The results indicated that the mean LST value increased by 2.32°C between 2000 and 2014. The rise of LST was consistent with the trend of rapid urbanization in Zhengzhou City, which resulted in sharp increases in impervious surfaces (IS) and substantial losses of vegetation cover. Furthermore, the investigation of LST and vegetation cover demonstrated that fractional vegetation cover (FVC) had a stronger negative effect on LST than normalized differential vegetation index (NDVI). In addition, LST was obviously correlated with LULC landscape patterns, and both landscape composition and spatial configuration affected UHI effects to varying degrees. This study not only illustrates a feasible way to investigate the relationship between LULC and urban thermal environment but also suggests some important measures to improve urban planning to reduce UHI effects for sustainable development.

1. Introduction

The process of rapid urbanization deeply affects biological diversity, ecosystem services, and regional environment [1–3]. Because of unprecedented urbanization, the issues of urban eco-environment have been attracting increased attention from the public, scientists, and urban managers [4, 5]. One of the acute problems is the UHI effect, where urban surfaces and atmospheric temperatures are warmer than the surrounding nonurban areas owing to transformation of land-cover types and anthropogenic-based heat [6, 7].

The UHI effect is a substantial issue, as it has several negative influences on urban environments and human health. The existing research has indicated that UHI effect markedly increases energy consumption [8], raises risks of heat and pollution-related mortality [9], deteriorates air pollution [10], and worsens living environment of city

dwellers [11]. Based on these impacts, the spatiotemporal patterns of UHI and the factors affecting its impacts have become popular topics and are being broadly researched across multiple disciplines [12–14]. Better understanding the UHI effect is vital to offer the scientific foundation for taking effective measures to mitigate urban thermal environment and promoting sustainable development of urban areas.

In the previous literature, the studies of UHI effect have been implemented by contrasting temperature observations of meteorological network within urban and rural areas surrounding the city [15–17]. However, these ground-based observations are too scattered, and some observation data are commonly unrepresentative of complex thermal environments, and it is hard to depend on field data alone to achieve accurate and enough information concerning the UHI [18, 19]. Consequently, with the fast development of RS technology in recent years, satellite image data have been applied universally in urban environment and climate research across the world. Satellite image data have become a strong means for UHI research because they provide a convenient and consistent mechanism for detecting the thermal features of urban surfaces [20–22]. The satellite remote-sensing images with a thermal infrared band can be transformed into land surface temperature (LST) to characterize an UHI [23, 24]. For example, Landsat TM/ETM+/OLI data have been widely applied to calculate the LST values for UHI effect studies [25, 26]. As a result, the SUHI is addressed in this study, and thermal band images of remote sensing are applied to determine LST.

In urban thermal environment studies, many documents have illustrated associations between LST and urban expansion, particularly changes in land-use types [27–29]. These studies have found that urban heat effect is substantially influenced by LULC change. Each type of urban land has its own thermal features and radiation characteristics that make different contributions to UHI effect [30, 31]. Urban impervious surfaces (IS), including asphalt roads and cement buildings, usually emit more heat and lead to higher temperatures, while areas with water and vegetation have lower temperatures [32]. Accordingly, like urban expansion and transformations in land-cover types, the urban thermal environment will change correspondingly. Numerous studies have found that natural landscapes, such as forests and croplands, are transformed into impervious surfaces during the process of urbanization [33, 34] and thus contribute to UHI effects. It has been suggested that a positive correlation exists between impervious surfaces (IS) and LST [35, 36]. In addition, as vegetated landscapes generally are beneficial for decreasing LST [37], some documents have stressed on comprehending the relationship among NDVI, FVC, and LST [38, 39]. These studies demonstrated that there is a negative relationship between NDVI, FVC, and LST at different spatial resolutions [32, 40], and the LST-NDVI relationship was more adapted to analyzing UHI effect in the summer [41]. In general, these previous documents have quantitatively explored the relationship between LULC changes and LST based on RS technology. However, urban LULC patches have various shapes and spatial configurations, and these factors may also influence the urban thermal environment. There are several UHI documents that have researched the impacts of landscape configuration and composition on LST from the perspective of landscape ecology. However, this approach fails to consider influence of other elements of landscape patterns, like patch shape, patch structure, and patch density, which may hide important details related to spatial distribution and add the uncertainties of analyzing the relationship between UHI and landscape patterns [42, 43]. Therefore, a more reasonable approach that studies the influence of landscapes of various sizes, spatial arrangements, and shapes on UHI effects would be needed.

To better comprehend urban landscape processes and dynamics, one should be able to precisely quantify its spatiotemporal variations [44, 45]. Landscape metrics, which are landscape ecological variations that can precisely describe spatial features of land surfaces [46, 47], have been employed to describe spatial patterns of urban landscapes and to clarify impacts of LULC patterns on urban heat effect in this study. Therefore, compared with the existing literature, this study has the following contributions. First, we investigate the relationship between NDVI, FVC, and LST, respectively, and discuss the correlation between different biophysical indicators and urban thermal environment. According to the research results, we can determine a suitable indicator for this study, making the research results more accurate. Second, we use the method of comprehensive analysis to investigate the relationship between landscape pattern and LST based on RS data, which provides an effective way to reveal the change process of urban ecology and thermal environment.

The main purpose of this research is to explore the impacts of landscape (LULC) patterns on UHI effects more accurately based on landscape metrics analysis and to investigate the landscape patterns (including composition and spatial configuration) of different LST zones to preferably comprehend the relationship between LULC and LST at a regional scale. We center on investigating the intensity of LST based on LULC using Landsat images and estimating the correlation among LST, fractional vegetation cover (FVC), NDVI, and urban landscape patterns to elaborate the related impacts of urbanization on urban thermal environment. Furthermore, remote-sensing data and landscape metrics provide new perspectives for scientists to research UHI effects, and the findings from this study can be used to recommend important policies for urban planning to mitigate UHI effects, which provides an effective way to reveal the process of urban ecological change. Thus, the main objectives of this research are as follows: (1) information regarding the spatiotemporal variation of LST and LULC of Zhengzhou City was investigated from 2000 to 2014; (2) a comparative analysis was implemented to explore the impacts of NDVI and FVC on LST using quantitative models; (3) the relationship between landscape patterns and LST was explored by statistical analysis. The sketch map of this study is given in Figure 1.

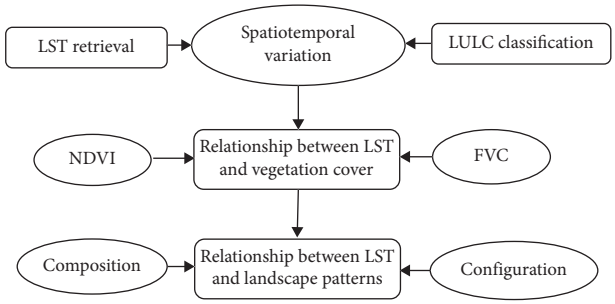

Figure 1: The sketch map of this study.

2. Materials and Methods

2.1. Study Area. Zhengzhou City is in the central inland area of China (112°42′E–114°14′E, 34°16′N–34°58′N) (Figure 2) and has an area of about 7446.2 km^2. The annual mean temperature of Zhengzhou city is approximately 14.4°C [48]. Like many other megacities in China, Zhengzhou City has been experiencing rapid urbanization and population growth in the past few decades. Based on local statistical data, from 2000 to 2014, Zhengzhou City's urbanization rate raised from 55.1% to 68.3%. This rapid land use process unavoidably led to urban environment degradation caused by UHI effect.

2.2. Data Sources and Preprocessing. In this study, available Landsat-7ETM+ (2000), Landsat-5TM (2006), and Landsat-8 OLI/TIRS (2014) images were collected from the USGS website (http://www.earthexplorer.usgs.gov), and these images were applied to establish time series data to acquire LULC information and to describe the heat environment of the entire area of Zhengzhou City. Additionally, each image was subjected to a series of preprocessing before LST retrieval, and these procedures mainly contained the radiometric calibration, atmospheric correction and geometrical distortions correction. Subsequently, all these images were resampled to 30 m to ensure correspondence to the resolution of multispectral bands [49]. The flowchart of this study is given in Figure 3.

2.3. Methods

2.3.1. Classification of LULC. The LULC maps of Zhengzhou City in 2000, 2006, and 2014 were obtained from Landsat imagery. The supervised classification and human-computer interactive interpretation were applied in ENVI 5.1. The urban landscape was classified into six categories: IS, water, bareland, farmland, forest, and grassland. The accuracy assessment of the classified LULC was implemented with 400 reference points that were generated to represent different LULC types of Zhengzhou City [50]. Therefore, the overall accuracy of LULC category was approximately over 86.6%, which met the requirements for this study.

2.3.2. LST Retrieval and Delineation of LST Intensity Zones. To date, several good retrieval algorithms of LST based on different data sources have been developed [51, 52]. In the research, the image-based method (IB) is applied to retrieve LST values because of its validity and simplicity [49]. Before retrieval of LST, a quadratic model was adopted to transform the digital number (DN) of Landsat TM/ETM + thermal infrared (TIR) band into radiant temperatures [53]:

$$L_\lambda = \text{gain} \times \text{QCAL} + \text{offset}, \quad (1)$$

where L_λ denotes the radiance of the thermal band pixel in $W/(\text{m}^2 \cdot \text{sr} \cdot \mu\text{m})$; gain denotes the slope of the radiance/DN conversion function; offset denotes the slope of the radiance/DN conversion; QCAL denotes the quantized calibrated pixel value in DN [21]. Then, the spectral radiance was transformed into the at-satellite brightness temperature [53], and equation (2) is as follows:

$$T_B = \frac{K_2}{\ln\left(1 + \left(K_1/L_\lambda\right)\right),} \quad (2)$$

where T_B denotes the effective at-satellite temperature in K; both K_1 and K_2 are prelaunch calibration constants (for Landsat-7, K_1 is 666.09 $W/(\text{m}^2 \cdot \text{sr} \cdot \mu\text{m})$and K_2 is 1282.71 K; for Landsat-5, K1 is 607.76 $W/(\text{m}^2 \cdot \text{sr} \cdot \mu\text{m})$ and K_2 is 1260.56 K; for Landsat-8, K_1 is 774.89 $W/(\text{m}^2 \cdot \text{sr} \cdot \mu\text{m})$ and K_2 is 1321.08 K).

In the research, considering the nature of LULC types, the vegetated areas (farmland, grassland, and forest), water bodies, impervious surfaces (IS), and bareland were given the values of 0.95, 0.9925, 0.923, and 0.92, separately [54–56]. Additionally, the emissivity-corrected land surface temperatures were calculated in equation (3) [54]:

$$\text{LST} = \frac{T_B}{1 + \left(\lambda \times T_B/\rho\right)\ln \varepsilon}, \quad (3)$$

where T_B equals at-satellite brightness temperature in degrees Kelvin; λ equals wavelength of emitted radiance ($\lambda = 11.5\,\mu$m, the center wavelength of Landsat TM Band 6 [32, 57], and 10.8 μm for Landsat OLI/TIRS Band 10 [58]); $\rho = h \times c/\sigma\,(1.438 \times 10^{-2}\,\text{mK})$, ρ = Boltzmann constant (1.38×10^{-23} J/K), h equals Planck's constant (6.626×10^{-34} Js),c equals velocity of light (2.998×10^8 m/s); and ε denotes the land surface emissivity. Then, the final LST values were transformed to degrees Celsius (°C).

According to the above information, it is inappropriate to directly compare the LST values or examine the variances of LST values over multiple years periods on account of the interannual variability of atmospheric conditions. Hence, the LST values was standardized in ArcGIS 10.2 software according to the data range (equation (4)), and the mean standard deviation (STD) means was used to separate the LST values into five zones (Table 1). These zones can be employed to analyze the spatial pattern and relationships of urban landscape metrics:

$$T_s = \frac{T_i - T_{\min}}{T_{\max -} T_{\min}}, \quad (4)$$

where T_s denotes the standardized LST value of a pixel, T_i denotes the initial LST value of pixel I, $T_{\max}$ denotes the maximum LST value, and $T_{\min}$ denote the minimum LST value.

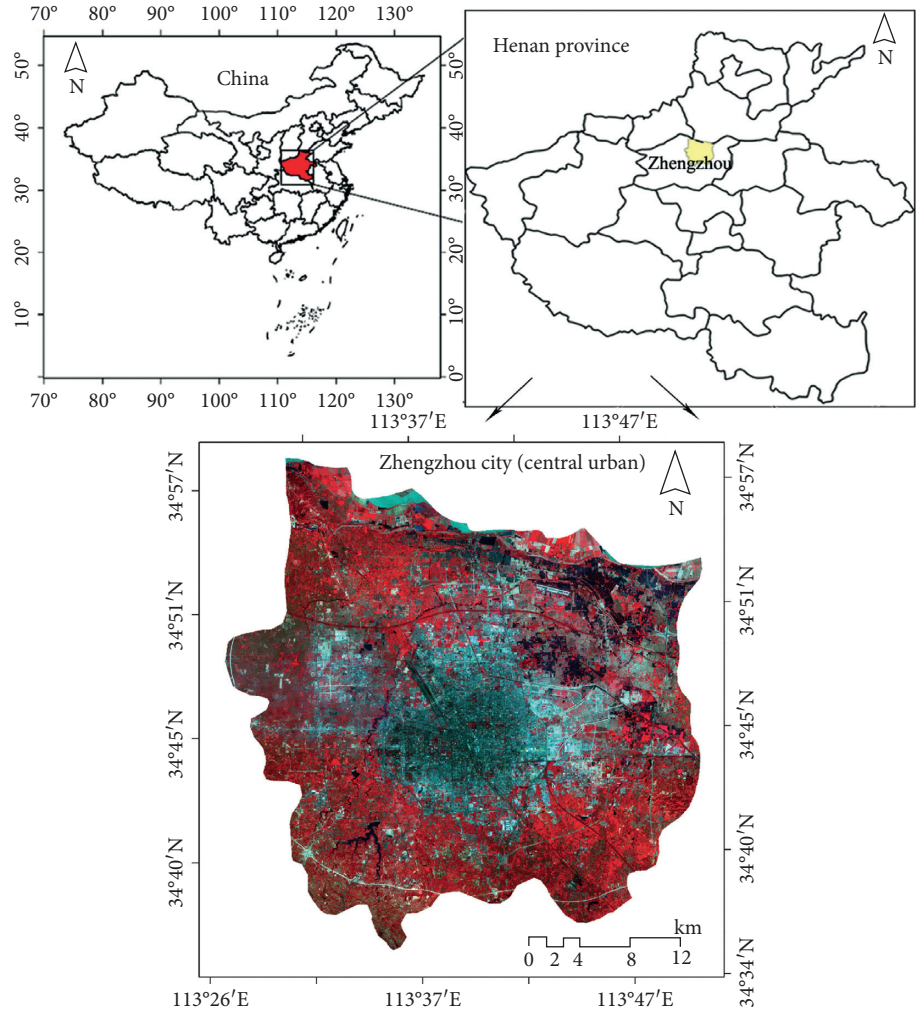

Figure 2: Location map of the study site.

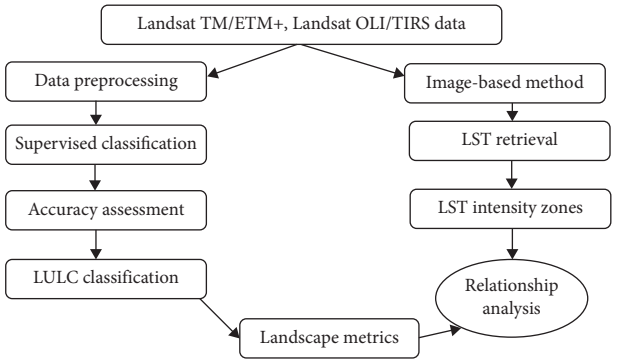

Figure 3: The flowchart of this study.

2.3.3. Computation of Biophysical Indices. The NDVI and FVC were applied as the key biophysical indicators. The NDVI was calculated as follows [59]:

$$\mathrm{NDVI} = \left(\frac{\rho_{\mathrm{NIR}} - \rho_{\mathrm{Red}}}{\rho_{\mathrm{NIR}} + \rho_{\mathrm{Red}}}\right), \tag{5}$$

where NIR denotes the reflectance of the near-infrared and RED denotes the reflectance of red bands.

Table 1: The classification of LST zones [4].

LST zones	Classification
Low	$T_S \le T_{mean} - \mathrm{std}$
Sub-low	$T_{mean} - \mathrm{std} < T_S \le T_{mean} - 0.5\mathrm{std}$
Medium	$T_{mean} - 0.5\mathrm{std} < T_S \le T_{mean} + 0.5\mathrm{std}$
Sub-high	$T_{mean} + 0.5\mathrm{std} < T_S \le T_{mean} + \mathrm{std}$
High	$T_S > T_{mean} + \mathrm{std}$

Note: T_S denotes the standardized LST value; T_{mean} denotes the mean standardized LST value; std denotes the standard deviation.

The FVC depicts the amount and nature of vegetation cover, and it depends on the NDVI as follows [60]:

$$\mathrm{FVC} = \left(\frac{\mathrm{NDVI}_i - \mathrm{NDVI}_s}{\mathrm{NDVI}_v - \mathrm{NDVI}_s}\right)^2, \tag{6}$$

where NDVI_i denotes NDVI value of a pixel I; NDVI_S denotes the NDVI value of pure soil, and the NDVI_V denotes the NDVI value of pure vegetation. To calculate accordant values of FVC, it needs to set pixels with $\mathrm{NDVI}_i > \mathrm{NDVI}_v$ to 1 and the pixels with $\mathrm{NDVI}_i < \mathrm{NDVI}_S$ to 0 [61, 62].

2.3.4. Calculation of Landscape Metrics. To quantify the relationship between urban landscape patterns and LST, a series of landscape metrics (including composition, shape, and configuration) was computed based on 5×5 pixel moving window in FRAGSTATS 4.2 software package. The metrics were chosen according to the principles of minimal redundancy [63–65]. Overall, six landscape-based metrics and eight class-based metrics were chosen to describe characteristics of landscape patterns (Table 2). In addition, the Pearson correlations between mean LST values and landscape metrics were calculated and employed to determine the impacts of land-use landscape patterns on the UHI.

3. Results

3.1. LULC Dynamics. The dynamics of LULC of Zhengzhou City during 2000 and 2014 are demonstrated in Figure 4. Zhengzhou City has experienced remarkable urbanization, and the land use/cover pattern changed considerably. According to the land-use types, the outcomes revealed that the area of IS increased from 133.2 km^2 to 282 km^2 in 2000–2006, and it increased by 130.7 km^2 in 2006–2014. The total increase was 279.5 km^2 over the 14-year period. Between 2000 and 2014, the total net loss of forest and farmland reached 25.07% and 24.07%, respectively, within the whole study area. While water had the smallest proportion of area, it declined from 3.22% in 2000 to 0.92% in 2014. The primary changes in urban LULC types occurred in the northwest and east of Zhengzhou City, which were the areas that underwent the sharpest urban expansion since 2000.

3.2. LST Patterns within Each LULC Category. Statistically, in 2000, the mean value of LST is 29.73°C, while the mean value of LST is 31.96°C in 2014. This result shows that the mean LST gradually increased by 2.23°C from 2000 to 2014 overall.

In addition, this research calculated the mean LST values for each LULC category between 2000 and 2014 (Figure 5). The results reflected that mean LSTs of the different types of landuse/landcover had clear differences. According to the mean LST values, it can be observed that impervious surfaces had a higher LST value, whereas forest and water had lower LST values during this study period. The impervious surfaces were linked to roads, buildings and dense populations, and thermal properties of these building materials, and anthropogenic heat sources made impervious surfaces become the hottest regions. Bareland and farmland had relatively higher mean LST values because the bareland class usually had little vegetation cover, while the LST of farmland was always influenced by its associated agricultural activities [67]. The forest class with high vegetation coverage has a lower LST because of the shading and evapotranspiration that occur within this class. Overall, the LULC categories with different thermal characteristics influenced the distribution of LST.

As shown in Figure 6, the spatial dynamics revealed that the LST values in urban areas were higher than that in the surrounding areas in 2000–2014. The sub-high and high zones are mainly distributed in the commercial districts of the central urban areas and in the industrial districts' northwest and south of Zhengzhou City. In comparison, the sub-low and low zones were found inside the urban areas and gradually had a scattered distribution. Meanwhile, the area of sub-high and high zones increased substantially, while the areas of the sub-low and low zones decreased sharply, which was due to the dramatic changes that occurred in the LULC patterns that greatly influenced the thermal environment. A large amount of farmland and other vegetation cover types have been converted into impervious surfaces and artificial buildings due to rapid urban expansion during this study period.

Table 3 shows the proportion of LULC categories of different LST zones from 2000 to 2014. The magnitude of the differences in zonal proportions associated with impervious surfaces was more pronounced in the medium zone and high zone, with an obvious increase between 2000 and 2014. However, the proportions declined in sub-high zone. One reason for this result may be the variations in the urban land use types, characterized by concrete surfaces interspersed with spotty patches of green parks and grasslands [45]. For the same reason, the proportion of grassland increased in all the zones from 2000 to 2014. However, the proportions of forest clearly declined in the low zone and sub-low zone, which was probably due to impervious surfaces replacing forest patches during rapid urbanization. In addition, it appeared that the proportion of farmland declined in the low and sub-low zones, but it increased in the high zones, which was on account of a combination of agricultural activities and seasonal weather impacts on LST.

3.3. Relationship among LST, NDVI, and FVC. NDVI and FVC have been regarded as two key biophysical parameters in thermal remote-sensing analyses. Previous studies have demonstrated that NDVI could be considered a representative indicator of land surface vegetation coverage [21, 68], whereas FVC is often applied to represent vegetation abundance. To better comprehend the effects of vegetation cover on UHI, we applied Regression function and Pearson correlation analysis to estimate the relationships among the LST, NDVI, and FVC. The results are shown in Table 4. A strong and negative correlation between FVC and LST can be observed, but there is a weak and negative correlation with NDVI across the entire range of values. This result shows that FVC is a better reflection of LST characteristics than the NDVI, and several studies also identified similar relationships among LST, NDVI, and FVC [61, 69]. Hence, in this study, FVC is more suitable for assessing the correlation between vegetation abundance and LST.

Figure 7 shows the spatial patterns of FVC in Zhengzhou City between 2000 and 2014. The city center exhibited lower FVC and higher LST, while the surrounding areas with a relatively higher FVC exhibited lower LST. This indicates that inverse trends in FVC and LST were observed. To further validate the results, we obtained the mean and SD zonal FVC shown in Table 5. Obviously, there was a decrease in the FVC value as the higher LST zone increased, which illustrated a clear correlation between FVC and LST.

Table 2: List of landscape metrics [62, 66].

Level	Classification	Metrics
Landscape	Composition	Patch density (PD)
	Shape	Largest patch index (LPI)
		Aggregation index (AI)
	Spatial arrangement	Contagion (CONTAG)
		Shannon diversity index (SHDI)
		Shannon evenness index (SHEI)
Class	Composition	Percent cover of class area (PLAND)
		Edge density (ED)
	Shape	Landscape shape index (LSI)
		Mean shape index (SHAPE_MN)
		Mean fractal dimension index (FRAC_MN)
	Spatial arrangement	Landscape division index (DIVISION)

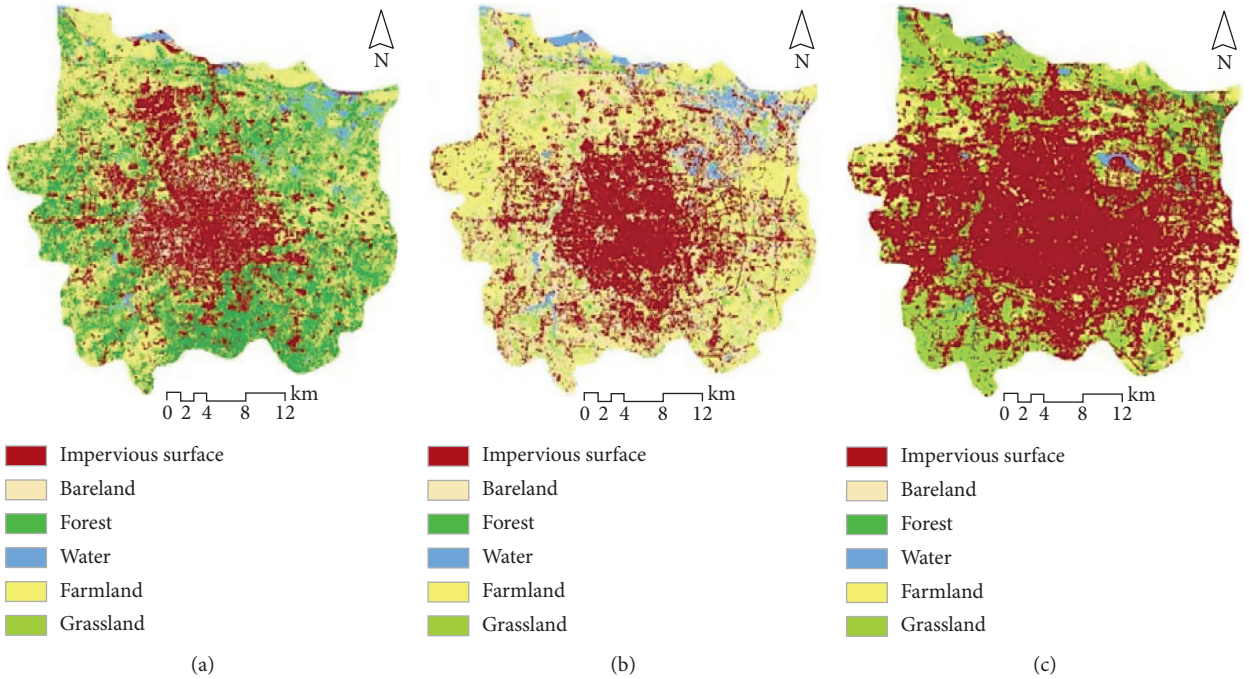

Figure 4: The LULC maps of Zhengzhou City in (a) 2000, (b) 2006, and (c) 2014.

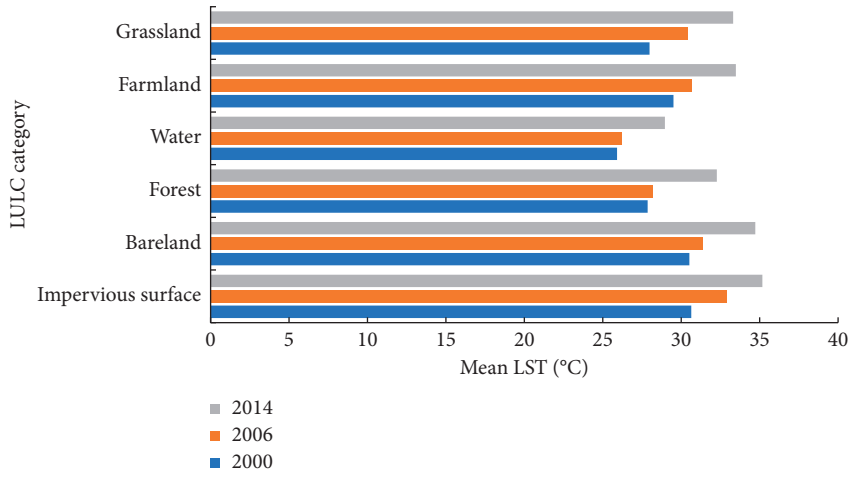

Figure 5: Mean LST values for the LULC categories from 2000 to 2014.

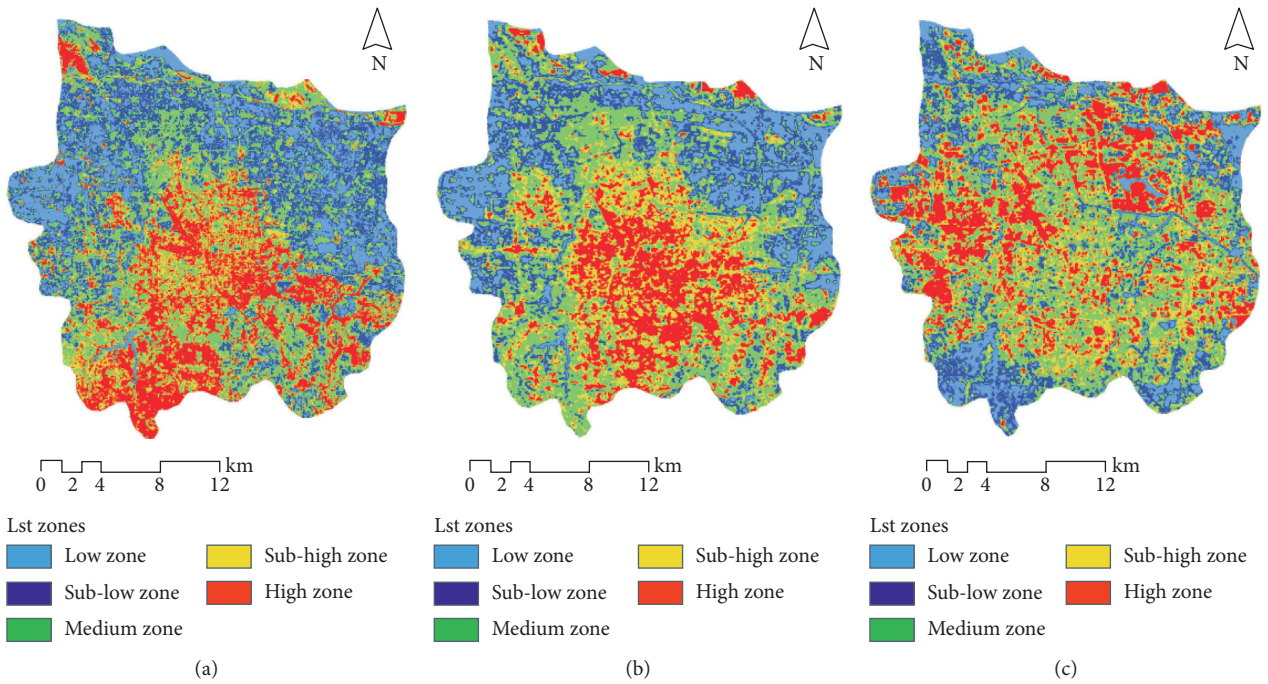

Figure 6: The spatial pattern of LST zones from 2000 to 2014. (a) 2000. (b) 2006. (c) 2014.

Table 3: The proportion of LULC types (%) of different LST zones from 2000 to 2014.

	Zone1			Zone2			Zone3			Zone4			Zone5		
	2000	2006	2014	2000	2006	2014	2000	2006	2014	2000	2006	2014	2000	2006	2014
Grassland	0.005	0.829	4.117	0.012	1.409	5.324	0.007	2.242	9.141	0.007	0.301	3.012	0.002	0.099	2.180
Farmland	3.345	6.117	2.161	8.703	4.939	1.625	3.376	9.159	3.223	4.471	5.111	2.254	1.078	4.322	4.222
IS	1.562	1.788	2.602	6.669	1.649	4.577	12.961	6.486	23.492	21.439	9.609	16.491	11.981	10.990	12.821
Forest	2.235	0.149	1.137	6.143	0.106	0.143	2.882	0.119	0.071	10.466	0.010	0.013	2.452	0.002	0.027
Water	0.019	2.645	0.774	0.068	0.379	0.032	0.028	0.193	0.033	0.008	0.041	0.019	0.001	0.028	0.051
Bareland	0.001	3.749	0.062	0.001	5.403	0.007	0.023	15.236	0.057	0.015	5.246	0.064	0.027	1.631	0.257
Total	7.167	15.281	10.855	21.598	13.887	11.71	19.281	33.437	36.021	36.409	20.32	21.855	15.543	17.074	19.559

Note: IS denotes impervious surface; Zone 1 denotes low LST zones; Zone 2 denotes sub-low LST zones; Zone 3 denotes medium LST zones; Zone 4 denotes sub-low LST zones; Zone 5 denotes low LST zones.

Table 4: The linear regression and correlation coefficients among LST, NDVI, and FVC.

	2000		2006		2014	
	NDVI	FVC	NDVI	FVC	NDVI	FVC
LST	$y = -1.03 + 0.69$ R^2: 0.55 r: -0.56^{**}	$y = -71.35x + 38.87$ R^2: 0.85 r: -0.79^{**}	$y = -0.31x + 0.64$ R^2: 0.64 r: -0.63^{**}	$y = -93.93x + 36.44$ R^2: 0.73 r: -0.82^{**}	$y = -0.32x + 0.64$ R^2: 0.72 r: -0.49^{**}	$y = -138.84x + 37.91$ R^2: 0.84 $r = -0.81^{**}$

Note: y denotes LST; x denotes FVC and NDVI; r denotes correlation coefficient; **Correlation denotes significancee at the 0.01 level.

Therefore, the changes in FVC well explained the impact of biophysical features on the SUHI pattern.

3.4. Relationship between Landscape Metrics and LST. As shown in Tables 6 and 7, clearly, bareland and water changed insignificantly on account of their scattered distributions and small patch sizes. The other four main LULC types, including farmland, forest, and grassland and impervious surface, accounted for the major components of the urban surface and had important effects on the UHI in Zhengzhou City. Thus, the landscape patterns of these four LULC types were considered and discussed in the statistical analysis of class-level metrics.

This research demonstrated that LST is not only related to landscape composition but also to spatial configurations at the landscape level. The LST is positively correlated with PD and CONTAG, indicating that landscapes with higher patch density and fewer contiguous patches will lead to high values of contagion, which results in enhancing the UHI

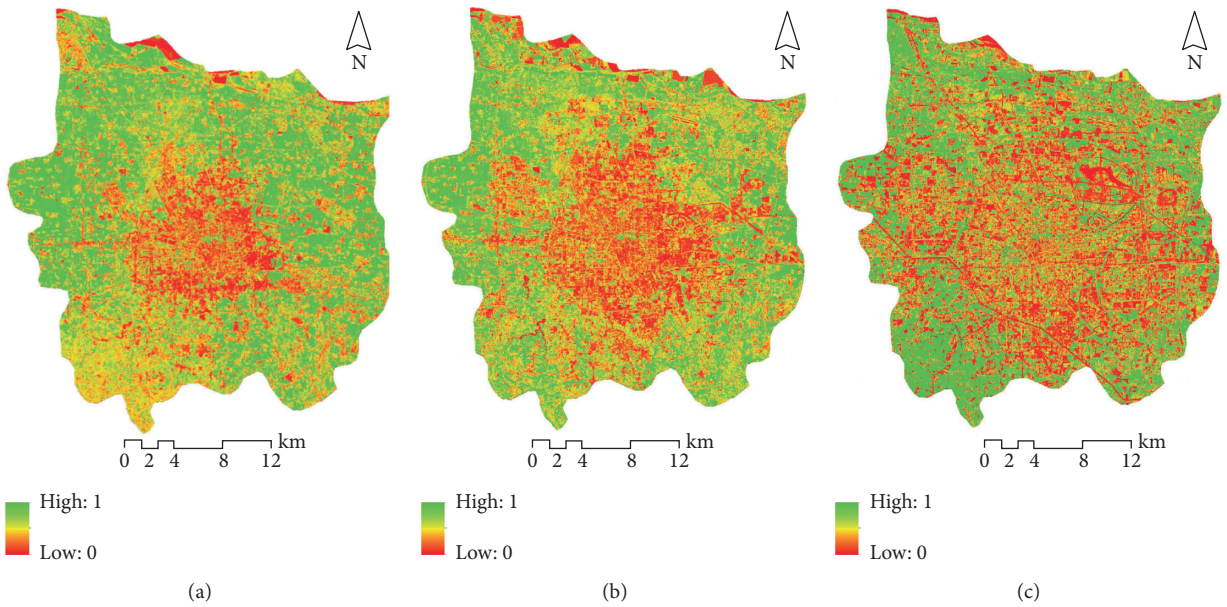

Figure 7: Spatial distribution of FVC from 2000 to 2014.

Table 5: Mean and SD zonal FVC derived from different LST zones.

Year	Item	Low zone	Sub-low zone	Medium zone	Sub-high zone	High zone
2000	Mean	0.637	0.587	0.473	0.358	0.297
	SD	0.205	0.158	0.161	0.147	0.122
2006	Mean	0.544	0.514	0.436	0.311	0.253
	SD	0.206	0.153	0.168	0.149	0.121
2014	Mean	0.634	0.605	0.417	0.305	0.221
	SD	0.257	0.214	0.208	0.227	0.174

Table 6: Correlation coefficients between landscape-level metrics and LST.

	AI	CONTAG	LPI	PD	SHDI	SHEI
2000	−0.354*	0.246*	−0.311*	0.391*	−0.451**	−0.408**
2006	0.193	0.372*	0.326*	0.639**	−0.534**	−0.496**
2014	0.179	0.458**	0.372*	0.665**	−0.560**	−0.535**

*Correlation denotes significance at the 0.05 level; **correlation denotes significance at the 0.01 level.

Table 7: Correlation coefficients between class-level metrics and LST.

		AI	DIVISION	ED	FRAC MN	LSI	PD	PLAND	SHAPE MN
Farmland	2000	−0.141	−0.541**	−0.206	−0.23*	−0.504**	−0.438**	−0.681**	−0.248*
	2006	−0.314*	−0.482**	−0.252	−0.356**	−0.542**	−0.368*	−0.581**	−0.127
	2014	−0.158	−0.396**	−0.309*	−0.38**	−0.527**	−0.341*	−0.655**	−0.122
Forest	2000	−0.229*	−0.51**	−0.292*	−0.185	−0.269*	−0.157	−0.685**	−0.288*
	2006	−0.245*	−0.648**	−0.272	−0.182	−0.127	−0.119	−0.757*	−0.124
	2014	−0.296*	−0.533**	−0.305*	−0.172	−0.355*	−0.137	−0.543*	−0.301*
Grassland	2000	−0.311*	−0.618**	−0.266	−0.371**	−0.047	−0.025	−0.685**	−0.223*
	2006	−0.215	−0.557**	−0.241	−0.246*	−0.173	−0.146	−0.638**	−0.314**
	2014	−0.102	−0.552**	−0.314*	−0.235*	−0.26*	−0.187	−0.603**	−0.432**
IS	2000	0.357**	−0.342*	0.258	0.342**	0.132	0.168	0.493**	0.308**
	2006	0.458**	−0.397*	0.255	0.494**	0.232*	0.129	0.625**	0.351**
	2014	0.523**	−0.413**	0.366*	0.559**	0.139	0.174	0.669**	0.614**

*Correlation denotes significance at the 0.05 level; **correlation denotes significant at the 0.01 level. IS denotes impervious surface.

effect and vice versa. However, SHDI and SHEI are negatively correlated with LST. Additionally, the correlation of LST with AI and LPI is unstable because of the changes in the shape and proportion of the urban landscape patterns. In general, these findings indicated that abundance of LULC categories and spatial configurations will contribute to mitigating the UHI effect.

As shown in Table 7, the LST was negatively correlated with AI, DIVISION, ED, FRAC MN, LSI, PD, PLAND, and SHAPE MN for farmland, forest, and grassland. However, the landscape metrics for impervious surfaces mainly had positive impacts on LST because of their thermal conductivity [62]. For the spatial configuration variables, it was indicated that higher aggregations of farmland, forest, and grassland patches could reduce UHI effect, while the aggregation of impervious surfaces could enhance the UHI effect. For the composition variables, it was implied that LST would be reduced with the increase of vegetation patches' percentage and density, while the increase of impervious surface patches proportion would intensify the thermal environment. For shape variables, it was demonstrated that the increase of vegetation patches in shape irregularity would enhance cooling effects, while the increase of impervious surface patches in the shape irregularity would intensify UHI effect. In addition, FRAC_MN of vegetation patches was negatively correlated with LST, which indicated better cooling effects of vegetation with improvement of shape complexity. However, the FRAC_MN of impervious surface patches was positively correlated with LST, which implied a reduction in UHI effects for impervious surface patches with less complex shapes.

4. Discussion

In view of the results offered by the spatial dynamics of LULC and LST zones, we identified some important features of the impacts of LULC on UHI effects during the process of urbanization. First, Zhengzhou City underwent rapid urbanization, as was evident based on the significant increase in spatial scale of IS from 2000 to 2014. These outcomes are consistent with findings of other previous literature [70, 71]. As the core city of central Henan urban agglomeration, Zhengzhou City has played an important role in regional development. Its urban areas have continued to grow since 2000, but after 2006, the expansion rate was much larger due to growth stimulation from planning policies at multiple levels. Second, LULC changes could result in drastic changes to the urban thermal environment in Zhengzhou City. The observed increasing trend of LST in study area was affected by landscape changes. In general, most of the expansion of built-up lands was produced from cropland and grassland transformations. A substantial portion of the natural surface landscape was replaced by traffic facilities, buildings, and asphalt roads. According to spatial pattern of the LST zones, the high LST zones generally were located within IS classes, but low LST zones were located within vegetated land-cover types. In addition, the investigation of LST and vegetation cover indicated that FVC had a stronger impact on LST than did NDVI. Hence, FVC was used to offer a better understanding of the correlation between LST and vegetation abundance in Zhengzhou City. Through the above analysis, we found that not all study areas are suitable for NDVI to reflect the relationship between vegetation cover and LST. Through comparative analysis, this study found FVC indicator that can accurately reflect the relationship between vegetation cover and LST, make up for the shortcomings of previous studies, and provide reference value for other areas. This finding can make up for the lack of using a single biophysical index in the previous research and provide reference value for other regions.

We also analyzed the relationship between urban landscape patterns and LST through landscape metrics and statistical analysis, which offered a new perspective for comprehending the evolution of the UHI effect. Our findings showed that spatial configuration and composition metrics were obviously correlated with LST, positive for vegetation landscape patches (including grassland and forest) and negative for impervious surfaces at the class level. These results are consistent with those of the other relevant researches [59, 62], for instance, Chen and Yu [72] identified obvious relationships between the LST and landscape patterns of impervious surfaces (positive) and vegetation cover (negative) in Guangzhou City of China. Overall, this research has indicated that integration methods of GIS, remote-sensing image classification technology, and landscape metrics are valid means to quantitatively analyze the relationship between landscape patterns and LST. These approaches can offer precise characteristics of the spatiotemporal change of urban thermal environment and some implications for other similar studies.

In addition, this research has some implications for policymakers and urban planners to mitigate the negative UHI effect. Our results showed that a higher proportion of impervious surface areas results in higher LST, while vegetation helps decrease LST and generates cool island effects by providing shade. In this context, one way to mitigate the UHI effect is to increase vegetation coverage, and it is important for the urban planners to consider the supply of more forested areas and green spaces in future development of Zhengzhou City. For example, the green roofs, small green space, and cool pavements should be encouraged to build. In addition, the findings of this research could help land-use managers optimize the spatial arrangements of urban landscapes to control UHI effects. It is recommended that regulating the spatial structure of impervious surface patches is a useful method to reduce UHI effects in future urban development. Meanwhile, continuous vegetation cover patches can help to optimize the spatial configurations diversity and obviously decrease LST values.

5. Conclusions

In this study, RS technology and geospatial approaches were applied to explore the effects of LULC changes on UHI. Using Zhengzhou City as a case study, the spatial features of urban landscape and thermal environment were investigated using the FVC and landscape metrics obtained from LULC

types and LST zones. (1) The results indicate that land-use changes of Zhengzhou City had a significant influence on its UHI effect, and the mean LST increased by 2.23°C from 2000 to 2014. Overall, this increasing trend of mean LST value is consistent with the rapid urbanization, which led to the sharp increase in impervious surfaces area and dramatic losses in vegetation coverage area. (2) The investigation of LST and FVC indicated that the FVC had an obvious negative relationship with urban thermal environment. (3) The relationships between LST and landscape patterns were investigated using landscape metrics and correlation analysis method. The findings indicated obviously different effects of LULC landscape patterns on LST, and it can be considered that impacts on LST is not only reflected in urban landscape composition but also in its shape and spatial configuration. Hence, it is noteworthy that the abundance of land-use categories and spatial configurations will contribute to mitigating UHI effects. In general, these findings suggest that some actions (e.g., increasing forests and grasslands, adjusting the spatial distribution of different landscape types, and optimizing the landscape configuration) could be taken to reduce the urban thermal environment to ensure a healthy and livable environment.

LST is one of the significant surface parameters applied for estimating the UHI effect, and this study indicated that different LULC types have complex relationship with LST. With the high-speed advancement of RS technology, we can investigate the effects of LULC on UHI at a finer spatial scale. In addition, there are some other factors including socio-economic transformation, climate change, and seasonal variation that may influence UHI effects at different levels. In the future, more attention should be given to the research of relationship between LST and urban landscape by comprehensive conditions analysis.

Abbreviations

LST: Land surface temperature
UHI: Urban heat island
FVC: Fractional vegetation cover
NDVI: Normalized difference vegetation index
IS: Impervious surface
LULC: Landuse/landcover.

Data Availability

In this study, (1) the available Landsat-7ETM+, Landsat-5TM, and Landsat-8OLI/TIRS images were collected from the US Geological Survey (USGS http://www.earthexplorer.usgs.gov) and were used to support the findings of this study; (2) the Biophysical Indices (NDVI and FVC) which were used to support the findings of this study were taken from Landsat images; (3) the Landscape Metrics is available from the LULC maps of Zhengzhou City.

Conflicts of Interest

The authors declare no conflicts of interest.

Acknowledgments

The research was sponsored by a grant of the Natural Sciences Foundation of China (Nos. 41501128 and 41430637) and support from the China Postdoctoral Science Foundation (2015M582181).

References

[1] M. Luck and J. Wu, "A gradient analysis of urban landscape pattern: a case study from the Phoenix metropolitan region, Arizona, USA," *Landscape Ecology*, vol. 17, no. 4, pp. 327–339, 2002.

[2] W. Chen, Y. Zhang, C. Wang, and W. Gao, "Evaluation of urbanization dynamics and its impacts on surface heat islands: a case study of Beijing, China," *Remote Sensing*, vol. 9, no. 5, p. 453, 2017.

[3] J. Yang, W. Liu, Y. Li, X. Li, and Q. Ge, "Simulating intraurban land use dynamics under multiple scenarios based on fuzzy cellular automata: a case study of Jinzhou district, Dalian," *Complexity*, vol. 2018, Article ID 7202985, 17 pages, 2018.

[4] H. B. Zhao, H. Zhang, C. H. Miao, X. Y. Ye, and M. Min, "Linking heat source–sink landscape patterns with analysis of urban heat islands: study on the fast-growing Zhengzhou city in Central China," *Remote Sensing*, vol. 10, pp. 1–22, 2018.

[5] J. Yang, S. H. Jin, X. M. Xiao et al., "Local climate zone ventilation and urban land surface temperatures: towards a performance-based and wind-sensitive planning proposal in megacities," *Sustainable Cities and Society*, vol. 47, pp. 1–11, 2019.

[6] D. J. Sailor and L. Lu, "A top-down methodology for developing diurnal and seasonal anthropogenic heating profiles for urban areas," *Atmospheric Environment*, vol. 38, no. 17, pp. 2737–2748, 2004.

[7] E. Kalnay and M. Cai, "Impact of urbanization and land-use change on climate," *Nature*, vol. 423, no. 6939, pp. 528–531, 2003.

[8] C. Yang, X. He, F. Yan et al., "Mapping the influence of land use/land cover changes on the urban heat island effect-a case study of Changchun, China," *Sustainability*, vol. 9, no. 2, pp. 1–17, 2017.

[9] P. A. Mirzaei, "Recent challenges in modeling of urban heat island," *Sustainable Cities and Society*, vol. 19, pp. 200–206, 2015.

[10] B. Stone Jr., "Urban heat and air pollution: an emerging role for planners in the climate change debate," *Journal of the American Planning Association*, vol. 71, no. 1, pp. 13–25, 2005.

[11] M. Dallimer, J. R. Rouquette, A. M. J. Skinner, P. R. Armsworth, L. M. Maltby, P. H. Warren et al., "Contrasting patterns in species richness of birds, butterflies and plants along riparian corridors in an urban landscape," *Diversity and Distributions*, vol. 18, no. 8, pp. 742–753, 2012.

[12] Q. Weng and D. A. Quattrochi, "Thermal remote sensing of urban areas: an introduction to the special issue," *Remote Sensing of Environment*, vol. 104, no. 2, pp. 119–122, 2006.

[13] J. S. Wilson, M. Clay, E. Martin, D. Stuckey, and K. Vedder-Risch, "Evaluating environmental influences of zoning in urban ecosystems with remote sensing," *Remote Sensing of Environment*, vol. 86, no. 3, pp. 303–321, 2003.

[14] C. S. B. Grimmond, M. Roth, T. R. Oke et al., "Climate and more sustainable cities: climate information for improved planning and management of cities (producers/capabilities perspective)," *Procedia Environmental Sciences*, vol. 1, pp. 247–274, 2010.

[15] P. I. Konstantinov, M. Y. Grishchenko, and M. I. Varentsov, "Mapping urban heat islands of arctic cities using combined data on field measurements and satellite images based on the example of the city of Apatity (Murmansk Oblast)," *Izvestiya, Atmospheric and Oceanic Physics*, vol. 51, no. 9, pp. 992–998, 2015.

[16] J. Yang, Y. C. Wang, X. M. Xiao, C. Jin, J. H. Xia, and X. M. Li, "Spatial differentiation of urban wind and thermal environment in different grid sizes," *Urban Climate*, vol. 28, Article ID 100458, 2019.

[17] T. R. Oke, "City size and the urban heat island," *Atmospheric Environment (1967)*, vol. 7, no. 8, pp. 769–779, 1973.

[18] V. Miles and I. Esau, "Seasonal and spatial characteristics of urban heat islands (UHIs) in northern west siberian cities," *Remote Sensing*, vol. 9, no. 10, pp. 1–15, 2017.

[19] C. J. Tomlinson, L. Chapman, J. E. Thornes, and C. J. Baker, "Derivation of Birmingham's summer surface urban heat island from MODIS satellite images," *International Journal of Climatology*, vol. 32, no. 2, pp. 214–224, 2012.

[20] R. Fabrizi, S. Bonafoni, and R. Biondi, "Satellite and ground-based sensors for the urban heat island analysis in the City of Rome," *Remote Sensing*, vol. 2, no. 5, pp. 1400–1415, 2010.

[21] Y. Xiong, S. Huang, F. Chen, H. Ye, C. Wang, and C. Zhu, "The impacts of rapid urbanization on the thermal environment: a remote sensing study of Guangzhou, south China," *Remote Sensing*, vol. 4, no. 7, pp. 2033–2056, 2012.

[22] W. Guo, X. Zhu, T. Hu, and L. Fan, "A multi-granularity parallel model for unified remote sensing image processing WebServices," *Transactions in GIS*, vol. 16, no. 6, pp. 845–866, 2012.

[23] J. Tsou, J. Zhuang, Y. Li, and Y. Zhang, "Urban heat island assessment using the Landsat 8 data: a case study in Shenzhen and Hong Kong," *Urban Science*, vol. 1, no. 1, pp. 2–22, 2017.

[24] J. A. Voogt and T. R. Oke, "Thermal remote sensing of urban climates," *Remote Sensing of Environment*, vol. 86, no. 3, pp. 370–384, 2003.

[25] D. R. Streutker, "A remote sensing study of the urban heat island of Houston, Texas," *International Journal of Remote Sensing*, vol. 23, no. 13, pp. 2595–2608, 2002.

[26] S. K. Jusuf, N. Wong, E. Hagen, R. Anggoro, and Y. Hong, "The influence of land use on the urban heat island in Singapore," *Habitat International*, vol. 31, pp. 232–242, 2007.

[27] H. Zhang, Z.-f. Qi, X.-y. Ye, Y.-b. Cai, W.-c. Ma, and M.-n. Chen, "Analysis of land use/land cover change, population shift, and their effects on spatiotemporal patterns of urban heat islands in metropolitan Shanghai, China," *Applied Geography*, vol. 44, pp. 121–133, 2013.

[28] H. Du, D. Wang, Y. Wang et al., "Influences of land cover types, meteorological conditions, anthropogenic heat and urban area on surface urban heat island in the Yangtze river delta urban agglomeration," *Science of the Total Environment*, vol. 571, pp. 461–470, 2016.

[29] J. Yang, J. Sun, Q. Ge, and X. Li, "Assessing the impacts of urbanization-associated green space on urban land surface temperature: a case study of Dalian, China," *Urban Forestry & Urban Greening*, vol. 22, pp. 1–10, 2017.

[30] D. J. Sailor, "Simulated urban climate response to modifications in surface albedo and vegetative cover," *Journal of Applied Meteorology*, vol. 34, no. 7, pp. 1694–1704, 1995.

[31] A. J. Arnfield, "Two decades of urban climate research: a review of turbulence, exchanges of energy and water, and the urban heat island," *International Journal of Climatology*, vol. 23, no. 1, pp. 1–26, 2003.

[32] Q. Weng, D. Lu, and J. Schubring, "Estimation of land surface temperature-vegetation abundance relationship for urban heat island studies," *Remote Sensing of Environment*, vol. 89, no. 4, pp. 467–483, 2004.

[33] C. Deng and C. Wu, "Examining the impacts of urban biophysical compositions on surface urban heat island: a spectral unmixing and thermal mixing approach," *Remote Sensing of Environment*, vol. 131, pp. 262–274, 2013.

[34] J. Song, S. Du, X. Feng, and L. Guo, "The relationships between landscape compositions and land surface temperature: quantifying their resolution sensitivity with spatial regression models," *Landscape and Urban Planning*, vol. 123, pp. 145–157, 2014.

[35] H. Q. Xu, "Quantitative analysis on the relationship of urban impervious surface with other components of the urban ecosystem," *Acta Ecologica Sinica*, vol. 29, pp. 2456–2462, 2009.

[36] Y. S. Lin, H. Q. Xu, and R. Zhou, "A study on urban impervious surface area and its relation with urban heat island: Quanzhou city, China," *Remote Sensing Technology & Application*, vol. 22, no. 1, pp. 14–16, 2007.

[37] S. Hamada and T. Ohta, "Seasonal variations in the cooling effect of urban green areas on surrounding urban areas," *Urban Forestry & Urban Greening*, vol. 9, no. 1, pp. 15–24, 2010.

[38] T. N. Carlson, R. R. Gillies, and E. M. Perry, "A method to make use of thermal infrared temperature and NDVI measurements to infer surface soil water content and fractional vegetation cover," *Remote Sensing Reviews*, vol. 9, no. 1-2, pp. 161–173, 1994.

[39] S. N. Goward, Y. Xue, and K. P. Czajkowski, "Evaluating land surface moisture conditions from the remotely sensed temperature/vegetation index measurements," *Remote Sensing of Environment*, vol. 79, no. 2-3, pp. 225–242, 2002.

[40] X. Zhang, R. C. Estoque, and Y. Murayama, "An urban heat island study in Nanchang City, China based on land surface temperature and social-ecological variables," *Sustainable Cities and Society*, vol. 32, pp. 557–568, 2017.

[41] F. Yuan and M. E. Bauer, "Comparison of impervious surface area and normalized difference vegetation index as indicators of surface urban heat island effects in landsat imagery," *Remote Sensing of Environment*, vol. 106, no. 3, pp. 375–386, 2007.

[42] W. Li, Q. Cao, K. Lang, and J. Wu, "Linking potential heat source and sink to urban heat island: heterogeneous effects of landscape pattern on land surface temperature," *Science of the Total Environment*, vol. 586, pp. 457–465, 2017.

[43] S. Brown, V. L. Versace, L. Laurenson, D. Ierodiaconou, J. Fawcett, and S. Salzman, "Assessment of spatiotemporal varying relationships between rainfall, land cover and surface water area using geographically weighted regression," *Environmental Modeling & Assessment*, vol. 17, no. 3, pp. 241–254, 2012.

[44] J. Wu, D. E. Jelinski, M. Luck, and P. T. Tueller, "Multiscale analysis of landscape heterogeneity: scale variance and pattern metrics," *Annals of GIS*, vol. 6, no. 1, pp. 6–19, 2000.

[45] Y. Zhang, I. O. A. Odeh, and E. Ramadan, "Assessment of land surface temperature in relation to landscape metrics and fractional vegetation cover in an urban/peri-urban region using landsat data," *International Journal of Remote Sensing*, vol. 34, no. 1, pp. 168–189, 2013.

[46] F. Herzog and A. Lausch, "Supplementing land-use statistics with landscape metrics: some methodological

considerations," *Environmental Monitoring and Assessment*, vol. 72, no. 1, pp. 37–50, 2001.

[47] P. S. Roy, H. Padalia, N. Chauhan et al., "Validation of geospatial model for biodiversity characterization at landscape level-a study in Andaman & Nicobar islands, India," *Ecological Modelling*, vol. 185, no. 2–4, pp. 349–369, 2005.

[48] M. Gong, S. Yin, X. Gu, Y. Xu, N. Jiang, and R. Zhang, "Refined 2013-based vehicle emission inventory and its spatial and temporal characteristics in Zhengzhou, China," *Science of The Total Environment*, vol. 599-600, pp. 1149–1159, 2017.

[49] Y.-y. Li, H. Zhang, and W. Kainz, "Monitoring patterns of urban heat islands of the fast-growing Shanghai metropolis, China: using time-series of landsat TM/ETM+ data," *International Journal of Applied Earth Observation and Geoinformation*, vol. 19, pp. 127–138, 2012.

[50] S. V. Stehman, "Sampling designs for accuracy assessment of land cover," *International Journal of Remote Sensing*, vol. 30, no. 20, pp. 5243–5272, 2009.

[51] Z. Qin, A. Karnieli, and P. Berliner, "A mono-window algorithm for retrieving land surface temperature from Landsat TM data and its application to the Israel-Egypt border region," *International Journal of Remote Sensing*, vol. 22, no. 18, pp. 3719–3746, 2001.

[52] J. C. Jiménez-Muñoz and J. A. Sobrino, "A generalized single channel method for retrieving land surface temperature from remote sensing data," *Journal of Geophysical Research*, vol. 108, no. D22, 2003.

[53] Landsat Project Science Office, *The Landsat-7 Science Data User's Handbook*, p. 186, Goddard Space Flight Center, NASA, Greenbelt, MD, USA, 2008, https://landsat.gsfc.nasa.gov/data/how-to-use-landsat-data/.

[54] D. A. Artis and W. H. Carnahan, "Survey of emissivity variability in thermography of urban areas," *Remote Sensing of Environment*, vol. 12, no. 4, pp. 313–329, 1982.

[55] K. Masuda, T. Takashima, and Y. Takayama, "Emissivity of pure and sea waters for the model sea surface in the infrared window regions," *Remote Sensing of Environment*, vol. 24, no. 2, pp. 313–329, 1988.

[56] J. E. Nichol, "High-resolution surface temperature patterns related to urban morphology in a tropical city: a satellite-based study," *Journal of Applied Meteorology*, vol. 35, no. 1, pp. 135–146, 1996.

[57] B. L. Markham and J. L. Barker, "Spectral characterization of the LANDSAT thematic mapper sensors," *International Journal of Remote Sensing*, vol. 6, no. 5, pp. 697–716, 1985.

[58] R. C. Estoque, Y. Murayama, and S. W. Myint, "Effects of landscape composition and pattern on land surface temperature: an urban heat island study in the megacities of Southeast Asia," *Science of the Total Environment*, vol. 577, pp. 349–359, 2017.

[59] K. P. Gallo and J. D. Tarpley, "The comparison of vegetation index and surface temperature composites for urban heat-island analysis," *International Journal of Remote Sensing*, vol. 17, no. 15, pp. 3071–3076, 1996.

[60] T. N. Carlson and D. A. Ripley, "On the relation between NDVI, fractional vegetation cover, and leaf area index," *Remote Sensing of Environment*, vol. 62, no. 3, pp. 241–252, 1997.

[61] J. A. Sobrino, J. C. Jiménez-Muñoz, and L. Paolini, "Land surface temperature retrieval from landsat TM 5," *Remote Sensing of Environment*, vol. 90, no. 4, pp. 434–440, 2004.

[62] H. Wu, L.-P. Ye, W.-Z. Shi, and K. C. Clarke, "Assessing the effects of land use spatial structure on urban heat islands using HJ-1B remote sensing imagery in Wuhan, China," *International Journal of Applied Earth Observation and Geoinformation*, vol. 32, no. 32, pp. 67–78, 2014.

[63] S.-W. Lee, S.-J. Hwang, S.-B. Lee, H.-S. Hwang, and H.-C. Sung, "Landscape ecological approach to the relationships of land use patterns in watersheds to water quality characteristics," *Landscape and Urban Planning*, vol. 92, no. 2, pp. 80–89, 2009.

[64] H. Li and J. Wu, "Use and misuse of landscape indices," *Landscape Ecology*, vol. 19, no. 4, pp. 389–399, 2004.

[65] K. RivaMurray, R. Riemann, P. Murdoch, J. M. Fischer, and R. Brightbill, "Landscape characteristics affecting streams in urbanizing regions of the Delaware River Basin (New Jersey, New York, and Pennsylvania, U.S.)," *Landscape Ecology*, vol. 25, no. 10, pp. 1489–1503, 2010.

[66] K. McGarigal, S. Cushman, M. Neel, and E. Ene, "FRAGSTATS: spatial pattern analysis program for categorical maps," University of Massachusetts, Amherst, MA, USA, 2002, http://www.umass.edu/landeco/research/fragstats/fragstats.html.

[67] K. Y. Vinnikov, Y. Yu, M. K. Rama Varma Raja, D. Tarpley, and M. D. Goldberg, "Diurnal-seasonal and weather-related variations of land surface temperature observed from geostationary satellites," *Geophysical Research Letters*, vol. 35, no. 22, pp. 1–6, 2008.

[68] Q. Weng, D. Lu, and B. Liang, "Urban surface biophysical descriptors and land surface temperature variations," *Photogrammetric Engineering & Remote Sensing*, vol. 72, no. 11, pp. 1275–1286, 2006.

[69] C. Song, "Spectral mixture analysis for subpixel vegetation fractions in the urban environment: how to incorporate endmember variability?" *Remote Sensing of Environment*, vol. 95, no. 2, pp. 248–263, 2005.

[70] B. Mu, A. L. Mayer, R. He, and G. Tian, "Land use dynamics and policy implications in Central China: a case study of Zhengzhou," *Cities*, vol. 58, pp. 39–49, 2016.

[71] J. Duan, X. Song, and X. Zhang, "Spatiotemporal variation of urban heat island in Zhengzhou city based on RS," *Chinese Journal of Applied Ecology*, vol. 22, no. 1, pp. 165–170, 2011.

[72] Y. Chen and S. Yu, "Impacts of urban landscape patterns on urban thermal variations in Guangzhou, China," *International Journal of Applied Earth Observation and Geoinformation*, vol. 54, pp. 65–71, 2017.